JOURNAL OF SPACECRAFT AND ROCKETS
Vol. 38, No. 5, September–October 2001

Comparison of Glideback and Flyback Boosters

M. R. Tetlow*
Adelaide University, Adelaide, South Australia 5005, Australia
U. M. Schöttle†
University of Stuttgart, Stuttgart 70550, Germany
and
G. M. Schneider‡
Adelaide University, Adelaide, South Australia 5005, Australia

The aim of the present study is to investigate alternative reusable launch vehicle concepts and to provide a comparison of two different vehicle configurations. The first concept vehicle uses airbreathing engines to perform a powered booster flyback mission, whereas the second concept employs only aerodynamic lift to achieve booster flyback. The optimization software employs a system parameter optimization, in conjunction with a trajectory parameter optimization, to calculate the optimal mass split and corresponding optimal trajectory. A reference mission is used to compare launch vehicle payloads for a fixed gross liftoff weight, assuming launch from Woomera Prohibited Area, South Australia. The payload for a vehicle using a powered flyback strategy is found to be considerably higher than that obtained by a vehicle employing an aerodynamic glide return flight.

Nomenclature

D	=	drag force, N
g_0	=	gravitational acceleration, m/s^2
h	=	altitude, m
I_{sp}	=	specific impulse, s
L	=	lift force, N
m	=	mass, kg
s	=	distance, m
v	=	velocity, m/s
Δv	=	velocity change, m/s

Introduction

RECENT years have seen a significant increase in the number of launch vehicles available for commercial payloads, resulting in a highly competitive launch vehicle market. With the exception of the space shuttle, all current launch vehicles, such as Ariane, Delta, H-2, Long March, etc., are expendable,[1] and all current launch vehicles are expensive to operate. This suggests that there is a need for a fully reusable launch vehicle that can provide a low-cost reliable launch service.

To contribute to the examination of future launch systems, the impact of mission requirements on launch vehicle design was examined. Two concepts of winged reusable launch vehicles, employing vertical takeoff and horizontal landing, were compared using different flyback strategies for the booster stage. The first concept used airbreathing engines for a powered return flight, whereas the second employed an unpowered aerodynamic glide to return to the launch site. The payload capability of the launch vehicle was optimized for a fixed gross liftoff weight (GLOW), yielding optimum stage mass split and the optimum trajectories for each concept.

The study assumed launch from Woomera Prohibited Area in South Australia. This launch site was chosen due to its remote location and the availability of the necessary infrastructure for a spaceport. Recent interest in Woomera by commercial launch companies, such as Kistler Aerospace Corporation, also justified the consideration of this launch site.

Received 30 November 2000; revision received 19 February 2001; accepted for publication 19 February 2001.

*Postgraduate Student, Department of Mechanical Engineering. Student Member AIAA.
†Senior Lecturer, Space Systems Institute. Senior Member AIAA.
‡Senior Lecturer, Department of Mechanical Engineering. Member AIAA.

Problem Description

An assessment of the commercial payloads expected for the next 10 years, carried out by the U.S. Federal Aviation Administration (FAA),[2] predicts that 76% of satellites launched into low Earth orbit (LEO) will have a mass of less than 800 kg. The geosynchronous Earth orbit (GEO) market will be dominated by two categories. It is expected that 36% of payloads will be between 1815 and 4082 kg and 42% between 4082 and 5443 kg, with the FAA prediction also indicating a growth in the number of satellites above 5443 kg in the GEO category. There are a number of launch vehicles that either already service the commercial payload market or are expected to in the near future. Table 1 shows a performance and cost comparison of these vehicles.

The high cost of these launch vehicles is either due to their expendability or their requirement for extensive refurbishment before launch. This cost has prompted much research into the development of fully reusable launch vehicles such as NASA's X-33 and X-34 technology demonstrators, the Future European Space Transportation Investigation Program (FESTIP)[3] study carried out in Europe, as well as investigations carried out in Japan, to mention a few. An indication of the cost reduction of reusability is displayed by the Kistler K1 reusable vehicle. According to Isakowitz,[1] it will cost 17 million U.S. dollars to launch a 4.5-ton payload to LEO, which is a significant reduction in cost compared to the values in Table 1.

Reference Mission

Considering the FAA study, it appears that a reusable launch vehicle needs to be developed to address the GEO payload market. The high LEO capability of such a launcher could also be used to service the International Space Station (ISS). It was decided to use an expendable kick stage to service the GEO market, due to the high mass of the second stage. A heavy second stage would require large volumes of propellant to achieve geostationary transfer orbit (GTO), significantly reducing its GTO payload capability. The two-stage system was thus optimized to achieve LEO.

The reference mission chosen was a circular mission inclined at an angle of 31.5 deg. The ascent trajectory was optimized for perigee insertion into a 94 × 466 km transfer orbit, with an allowance made for the fuel required to circularize to a 466-km circular orbit. A similar mission was used by Freeman et al.[4] for a conceptual design of a piloted launch vehicle, providing a base for comparison.

The payload capability for GTO was based on a 466 × 36,000 km altitude orbit. In this case, the payload for the 466-km circular orbit was used as the initial mass of the expendable kick stage and payload. The required fuel and structure weight for the kick stage was

Table 1 Launch vehicle comparison[1]

Name	Payload GLOW, tons	Payload LEO, kg	Payload GTO, kg	Cost, $ million (U.S.)
Ariane 5	737	16,000	6,800	150–180
Delta IV	733	19,200	10,843	140–170
Titan IV	860	17,700	14,110	196–248
Shuttle	2,040	16,050	——	300
H2A	406	8,400	4,100	165–170

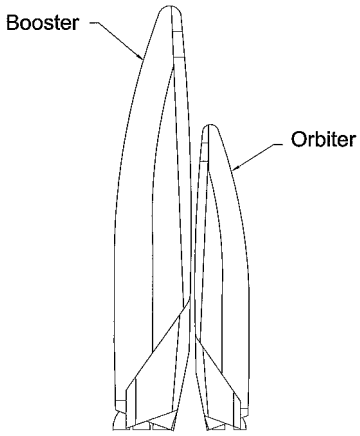

Fig. 1 Concept vehicle.

calculated using a structural coefficient of 15% and an I_{sp} value of 324 s (Ref. 1) for the propulsion system. It was also assumed that the payload alone would perform the inclination change from the 31.5-deg GTO to a 0-deg GEO.

The powered booster flyback in concept 1 assumed an aerodynamic turning glide flight until reaching subsonic cruise conditions. The remainder of the return flight was performed at cruise conditions powered by airbreathing engines. The assumed cruise conditions were a velocity of 270 m/s, a flight-path angle of 0 deg, and an altitude of 12,500 m. The end of the cruise flight was taken to be at cruise conditions over the landing site. Concept 2 (unpowered booster flyback) employed only an aerodynamic glide flight to return to the launch site. In this case the vehicle was assumed to land at the launch site with a velocity of 120 m/s, at the end of the cruise flight.

Concept Vehicle

The unpiloted concept vehicles discussed in this paper had a GLOW of 1400 tons. This value was chosen to enable the vehicles to launch approximately 20 tons into LEO, thereby allowing them to address the GEO market requirements discussed by Middleton.[2]

The vehicles consisted of two winged stages that operated in parallel during launch and initial ascent (Fig. 1). A cross-feed fuel system was employed to allow the orbiter to use propellants stored in the booster during mated flight. This would minimize the structural mass of the orbiter stage, thereby reducing the mass that had to be accelerated to the final orbit. A cross-feed system was also chosen because it was found to be optimal for a two-stage vehicle design.[3] The mated vehicle employed 11 liquid oxygen (LOX)/kerosene rocket engines for the ascent flight, providing a thrust-to-weight ratio of approximately 1.2 at launch. The number of rocket engines on each stage depended on the stage size. The powered return vehicle concept also employed two or three kerosene airbreathing engines for flyback, depending on the size of the booster stage.

Although a winged orbiter was not necessary, it would provide greater flexibility for the reentry mission as opposed to a ballistic reentry vehicle. A winged reentry vehicle would, thus, be advisable for a launch system that required a short turn around time. The orbiter conceived had the capability to land with its full launch payload, thereby enabling the vehicle to return a payload from orbit and also to avoid the payload having to be dumped in the event of an aborted launch.

Simulation and Optimization Techniques

The simulation technique employed a point mass, rigid-body dynamic model. The Earth was modeled as a rotating sphere with a Newtonian approximation of its gravitational field. A static atmosphere model, similar to the U.S. standard atmosphere, was used with no wind model. The three-degree-of-freedom dynamics equations were integrated using a fourth-order Runge–Kutta numerical integration technique.

Mass Modeling

Statistical mass modeling was employed to calculate the vehicle subsystem masses. A least-square curve fitting technique was used to linearize statistical mass data, which could be chosen by the launch vehicle designer. This choice allowed the designer to choose data perceived to have a similar technology level to the vehicle being considered. The mass model could also be scaled up or down, by a factor, to represent a change in technology level. Subsystem masses m_i were calculated using the statistical data in the form shown in Eq. (1):

$$m = \sum_{i=1}^{n} m_i = \sum_{i=1}^{n} A_i \cdot x_i^{B_i} \tag{1}$$

where A_i and B_i are the coefficients that define the technology, with respect to property x, of the subsystem. For example, the mass of the oxygen tank, m_{oxtnk}, is determined by the required tank volume x_{oxtnk} using a statistically determined, logarithmic relationship defined by A_1 and B_1. The vehicle was also scaled to match the shape and form of FESTIP Study System Concept (FSSC) 16 (Ref. 3).

Vehicle sizing was calculated from the required vehicle tank volume, including a 4% reserve. Assumptions had to be made regarding the mass of the nonstructural kerosene tanks, due to the lack of available data. The kerosene tanks were assumed to have the same mass fraction as that of the oxygen tanks. Because kerosene can be stored at lower pressures than oxygen and kerosene tanks can be manufactured from composite materials,[5] this assumption was considered to be conservative but satisfactory.

The mass of the fuel required for flyback of the powered return concept was calculated using the relationship shown by Eq. (2)

$$\Delta s = (L/D)\left[\left(v_1^2 - v_2^2\right)/2g_0 + h_1 - h_2 + I_{sp} v_2 \ln(m_1/m_2)\right] \tag{2}$$

The indices 1 and 2 represent conditions at the end of the optimized aerodynamic glide trajectory (beginning of cruise flight) and at the end of cruise flight, respectively. The propellant consumed during flyback was the difference between m_1 and m_2.

Although the statistical nature of the mass data should provide relatively accurate mass estimates, an uncertainty factor of approximately 10% was also included to account for mass errors. The 10% uncertainty factor was taken from the value used in the Ariane-X vehicle study.[6]

Aerodynamic Modeling

The aerodynamics of the vehicle were modeled as a table of lift and drag coefficients for given Mach numbers and angles of attack. These values were then interpolated using a spline function to produce a continuous function that described the aerodynamics of the vehicle.

The aerodynamic data were taken from the aerodynamic model of the Ariane-X concept vehicle[6] and then scaled to represent the aerodynamics of the FSSC-1 concept vehicle in the hypersonic region.[3] This scaling resulted in an optimistic maximum lift-to-drag ratio of 7 at a Mach number of 0.9.

Propulsion Systems

The propulsion systems chosen for this study included both rocket and airbreathing systems, depending on the configuration being considered and the flight regime. The core rocket engines used for the ascent were the Aerojet AJ26 series engines. These engines are modified Russian NK33 and NK43 engines, as used on the Russian Lunar program. The modifications made by Aerojet include updated

electronics, igniters, electronic controller, actuated control valves, and ±6-deg gimbaling.[7]

The rocket engines used on the booster stages were the Aerojet AJ26-59 engines, which have an I_{sp} value of 331.3 s in vacuum and 297.2 s at sea level. They weigh 1459 kg and produce 1.68 MN of thrust in vacuum and 1.51 MN at sea level. These engines are suited to low-altitude flight and have an expansion ratio of 27. The orbiter was equipped with AJ26-60 engines, which have an I_{sp} value of 345.3 s in vacuum. They produce 1.75 MN of thrust in vacuum and weigh 1505 kg. These engines are suited to high-altitude flight and have an expansion ratio of 80 (Ref. 7). Because the mass of the AJ26 engines is known,[7] it was not determined using the statistical mass analysis approach, but was simply calculated from the number of engines on the stage.

The airbreathing propulsion system used for flyback was based on the performance of the M88-35 turbojet engine. The mass for each engine was estimated to be 750 kg (Ref. 3). Without afterburners, this engine can produce 60 kN of thrust with a fuel consumption of 80 kg/kN · h.

The turbojet engines were not used during the ascent phase due to operational constraints. From an optimization point of view, turbojet operation during ascent increased the payload capability; however, the added complexity of advanced intake nozzles made it an unrealistic proposal. For this reason, the turbojets were only activated during subsonic cruise conditions in the flyback phase.

Previous concept vehicles such as Sänger[6] used airbreathing propulsion systems during ascent, descent turn flight,[6] and cruise flight, thereby suggesting that an engine operating in the higher Mach numbers is optimal. However, it was also discovered that the propulsion system should be throttled to produce only a fraction of its possible thrust during the supersonic descent phase.[6] Further more Sänger used the airbreathing engines for ascent and, thus, already had high-speed engines for use during descent. From the results of this study, it was decided that high-speed airbreathing engines were not required. Lighter, subsonic turbojet engines were, therefore, employed during cruise flight.

Optimization Technique

The optimization software used was developed at the Space Systems Institute in Stuttgart, Germany, and is described by Rahn et al.[6] The task was formulated as a nonlinear programming problem that was solved by a sequential quadratic optimization algorithm employing central difference gradient calculations. The chosen approach combined both optimization and design steps for the development of a launch vehicle. The payload was optimized for given staging conditions, which were then varied to obtain a trend toward the optimum staging conditions.

The mission was broken into three flight phases that had different parameter sets and were optimized independently to achieve a solution. Phase 1 was the ascent of the mated configuration, and it employed three parameters to describe the flight profile consisting of an initial pitch maneuver followed by a gravity turn. The three parameters used were thrust vector angle, duration of the pitching maneuver, and the launch azimuth. The target constraints were specified staging velocities and flight-path angles. Phase 2 was the booster stage flyback, and it was controlled by 16 optimization parameters, the first 12 being angle-of-attack control parameters and the remaining 4 being bank angle control parameters. The phase terminated when cruise flight (concept 1) or glide phase (concept 2) conditions were reached. Finally, phase 3, which was the orbiter ascent flight, was optimized with respect to five angle of attack parameters defining thrust angles. This phase terminated at the required altitude, velocity, and flight-path angle of the transfer orbit.

Results

Staging Conditions

The staging conditions play a significant role in the determination of an optimal trajectory for a given mission. Hence, it is important to perform staging at optimal conditions to maximize the payload. A number of optimization runs were performed on the orbiter stage using different staging flight-path angles, velocities, and altitudes to try to determine an initial estimate for the optimum staging conditions. A mass of 450 tons was used with an initial thrust to weight ratio of 1.2. According to Schöttle,[8] the optimal flight-path angle is between 7.5 and 20 deg for staging velocities between 2 and 3.5 km/s. There is a slight shift toward lower flight-path angles for an increase in staging velocity and staging altitude.

Table 2 Vehicle comparison[a]

Parameter	Value		
Staging velocity, m/s	2,500	3,000	3,500
Staging flight-path angle, deg	15	10	8
Staging altitude, km	59.8	62.8	70.0
Booster mass, tons	1,064	1,123	1,182
Booster propellant, tons	979	1,039	1,093
Orbiter mass, tons	336	277	218
Orbiter propellant, tons	298	209	184
Flyback distance, km	682	841	1,064
Maximum load factor, *g*	3.5	3.6	3.6
Number of airbreathers	2	2	3
Payload, ISS, kg	17,943	21,693	20,822
Payload, GTO, kg	5,793	7,005	6,723

[a]Mission, using powered booster flyback.

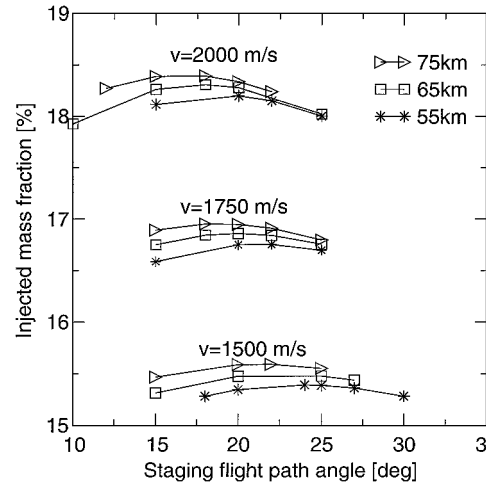

Fig. 2 Staging condition comparison.

The results displayed in Fig. 2 show a similar trend to those seen in Ref. 8, which used higher-energy cryogenic propellants. The injected mass fraction is shown to increase with an increase in staging velocity and altitude. The staging flight-path angle is shown to have an optimal value around 20 deg with a shift to lower flight-path angles with an increase in staging velocity and altitude. This investigation serves the purpose of displaying the similarities between the present study and the one conducted by Schöttle.[8] It suggests that the results obtained by Schöttle[8] can be used as a guide to the optimal staging conditions for the present study. The results also extended the work performed by Schöttle[8] to include lower staging velocities.

Concept 1: Powered Booster

The first concept considered was a two-stage, winged vehicle in a parallel configuration, employing a powered booster return flight. The booster flyback was achieved using airbreathing propulsion. The reason a powered return flight was proposed was to allow high staging velocities that were seen in Fig. 2 to allow higher injection mass fractions. Three different staging conditions were optimized to determine the design point for the configuration. The results from the optimizations, shown in Table 2, indicate that the optimum staging condition for a vehicle of this configuration is at approximately 3000 m/s.

Figure 2 showed that the higher the staging velocity is, the higher the injected mass fraction. It is also obvious that the higher the staging velocity the higher the booster mass, due to the requirement for larger propellant tanks. This higher mass would require a larger volume of propellant for the flyback maneuver. Another

factor contributing to the vehicle becoming heavier for higher staging velocities is the greater number of turbojet engines required to overcome aerodynamic drag during the return flight. A bigger vehicle would produce more aerodynamic drag during flight, due to the increased surface area. For the vehicle staging at 3000 m/s, only two turbojet engines would be required for flyback, whereas for a higher staging velocity of 3500 m/s, three turbojet engines would be required.

Table 2 shows a relatively small difference between the payload for a 3000 m/s staging velocity and that for a 3500 m/s staging velocity. This may indicate that the payload is not highly sensitive to staging velocity in the region of the optimum value. In this region, therefore, the design of a commercial launch vehicle may be dominated by the operational constraints instead of the payload capability.

The optimal staging velocity obtained in the present study was similar to the value of 3200 m/s obtained by Rahn et al.[6] for the optimal staging velocity of the Ariane-X concept vehicle. The Ariane-X vehicle also displayed a relatively small range of payload variation around the optimum staging velocity value.

The mass model employed for the present study used the landing mass of the vehicle to calculate the required mass of the wings. It considered a maximum load factor of 3.75 *g* for a pull-up maneuver before landing. Provided the loading during the flight was kept below 3.75 *g*, no wing strengthening was included. An investigation was performed using the 3000 m/s staging velocity concept vehicle to determine the effect on the payload of higher wing loads during the aerodynamic turn.

The mission was first optimized to allow a 3.6-*g* turn during flight, yielding a payload of 21,693 kg. A comparison mission was then optimized to allow a 4.6-*g* turn, yielding a payload of 21,827 kg. Hence, the difference in payload is 134 kg. The difference in mass between a wing designed to withstand a 3.75-*g* load during landing and one designed to withstand a 4.6-*g* turn during the return flight, was calculated to be 621 kg. Clearly, it is thus not optimal for this vehicle to perform high load turns during flight, because the extra mass required by the wing to support the turning load would outweigh the payload advantage from such a turn.

A result noted for the 2500-m/s staging velocity indicated that the vehicle did not have to execute a turn during its descent flight. Only a small difference in fuel consumption was noted for a trajectory that included a turn during its descent and one that descended in the ascent plane and then executed a sharp turn at cruise conditions.

Design Point Vehicle

The design point for this vehicle concept was a staging velocity of 3000 m/s, flight-path angle of 10 deg, and altitude of 62.8 km. The vehicle would consist of a 1123-ton booster stage employing nine AJ26-59 rocket engines and a 277-ton orbiter stage having two AJ26-60 rocket engines. It would operate in parallel during phase 1, employing a cross-feed fuel system to enable the orbiter to use propellants stored in the booster. The booster would require a return flight of 841 km, during which it would consume 7706 kg of fuel. It would also require two M88-35 turbojet engines to overcome drag during cruise flight.

As Fig. 3 shows, the vehicle would fly in the mated configuration for 186 s before separation. The orbiter would then switch to its own tanks and continue the ascent to the required orbit of 94 × 466 km. The booster would perform a coast phase while in the upper atmosphere with an angle of attack of 40 deg and a bank angle of −60 deg. The reason for this would be to perform as much of a turn and braking maneuver as possible while in the low-density atmospheric region. After approximately 330 s, the booster would perform a controlled braking and turning maneuver to obtain a heading toward the launch site and to achieve cruise conditions. Once cruise conditions had been reached, the airbreathing engines would be started, propelling the vehicle back to the launch site (not shown in figures).

From Fig. 4, note that the ascent phases of the booster and orbiter show a distinct exponential velocity increase due to the thrust increasing and vehicle mass decreasing during ascent. Figure 4 also shows the velocity of the booster would remain relatively constant,

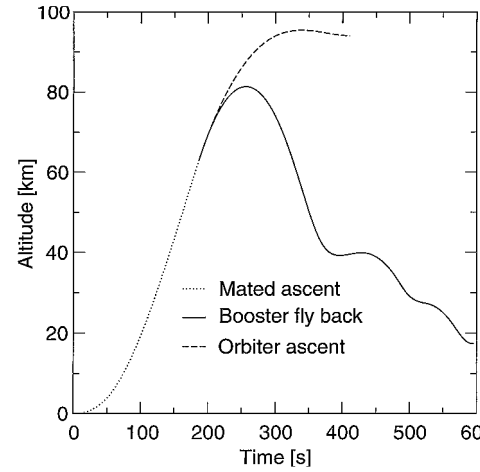

Fig. 3 Powered booster altitude profile.

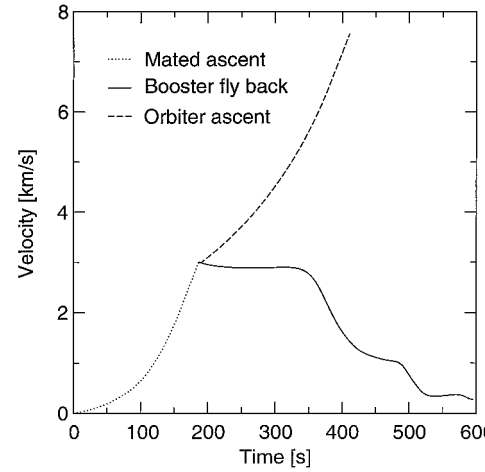

Fig. 4 Powered booster velocity profile.

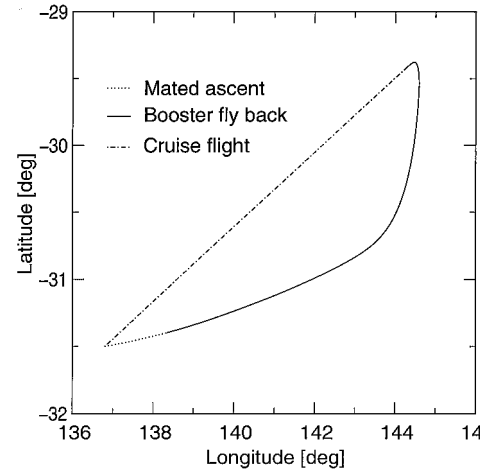

Fig. 5 Powered booster ground track.

around a value of 3000 m/s, for the first 180 s after separation. The absence of deceleration would be due to the low atmospheric density during this flight time, producing low aerodynamic forces on the vehicle. The ascent of the orbiter would have to be throttled during the last 30 s of flight to avoid load factors above 3.5 *g*.

Figure 5 shows a significant heading change close to the termination of the optimization. The reason for this is that there would be a high lift force at that altitude due to the high atmospheric density. It would also be a suitable time to execute a turn maneuver because the velocity of the booster would be relatively low, thereby resulting in a lower load factor during the turn.

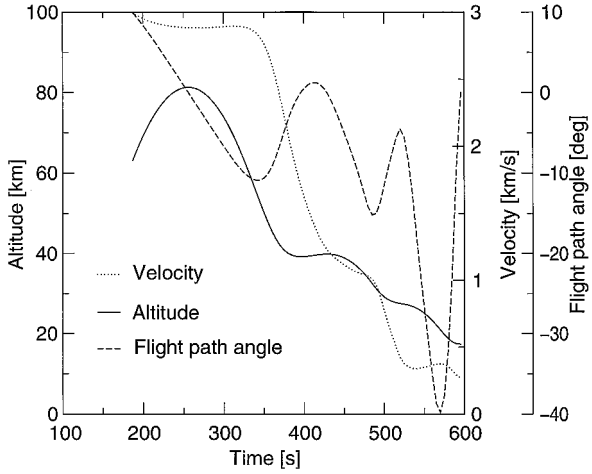

Fig. 6 Powered booster flyback mission.

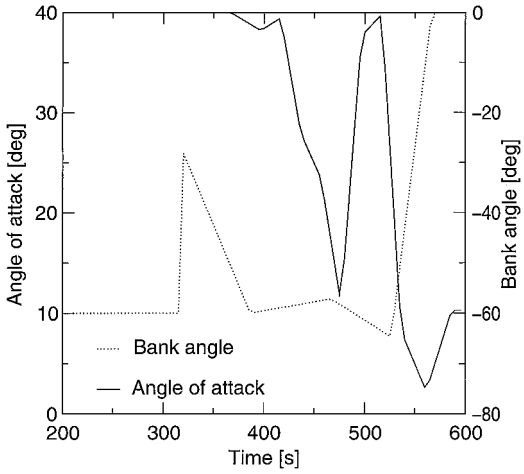

Fig. 7 Powered booster control parameters.

It can be seen from Fig. 5 that from staging to approximately 144° longitude, the booster would follow the ascent plane instead of executing a turn. Although there would be a high bank angle and angle of attack, the low atmospheric density of the upper atmosphere would produce little turning force.

From Fig. 6, it can be seen that the booster would climb to an altitude of 81 km before beginning its descent. At this high altitude, the lift forces on the vehicle would be low, typically in the range of 23 kN, thereby making control less effective in this area. This was evident by a relatively low sensitivity to control parameters in this flight regime.

The optimization was performed with the constraint of achieving a cruise velocity of 270 m/s and a flight-path angle of 0 deg at the termination of the simulation. A final altitude was not specified as an optimization constraint to allow more freedom of optimization. Provided the termination was above the specified cruise altitude, the solution was accepted. The vehicle was assumed to descend slowly at cruise conditions until it reached the required cruise altitude of 12,500 m. This accounted for the difference between the altitude at which the simulation terminated and the required cruise altitude.

In Fig. 7, note that the bank angle control parameter would start at a value of −60 deg. The reason for the −60-deg bank angle would be to perform as much of a heading change as possible during this flight period. Initially, an optimization parameter was used in this early flight region, but it proved problematic to the optimizer due to low optimization sensitivity to the parameter. It was, thus, decided to use a constant value for the angle of attack and bank angle until the aerodynamic forces became significant enough to allow stable optimization.

From Fig. 7, note that once the optimization for the bank angle parameters was activated, at 330 s, the bank angle jumped to a value of approximately −28 deg. This jump may indicate that the bank angle assumed before the optimization process started could have been reduced to a value of around −30 deg. The peak in the angle of attack, at around 500 s, would be required to create sufficient lift for the vehicle while it was at the maximum bank angle of −60 deg.

Table 3 Vehicle comparison for glideback booster[a]

Parameter	Value		
Staging velocity, m/s	1,000	1,100	1,200
Staging flight-path angle, deg	27	27	27
Staging altitude, km	24.6	30.62	34.0
Booster mass, tons	729	770	799
Booster propellant, tons	668	708	736
Orbiter mass, tons	671	630	601
Orbiter propellant, tons	588	549	521
Flyback distance, km	69.5	80.9	92.28
Maximum load factor, *g*	2.7	2.6	3.4
Payload, ISS, kg	13,471	14,079	14,709
Payload, GTO, kg	4,358	4,546	4,749

[a]Gliding booster flyback mission.

Concept 2: Glideback Booster

The following concept would use only aerodynamic lift to achieve the booster stage return flight. Again, this concept vehicle was optimized using three different staging conditions, the results of which are shown in Table 3.

The staging flight-path angle was optimized for the ascent phases only. The optimum flight-path angle, with respect to ascent, was then used to determine if a return glide to the launch site was possible. The maximum distance that the vehicle could glide was determined using Eq. (2). Clearly, the mass before and after the return flight was the same, thereby eliminating the log term.

As for the powered return flight concept vehicle, the stopping criteria for the optimization was a flight-path angle of 0 deg and a velocity of 270 m/s. This velocity was used as the initial velocity in Eq. (2), and the final velocity was taken to be 120 m/s, which was the assumed landing velocity. The altitude at the termination of simulation was used as the initial altitude in Eq. (2) and always had a value above 10 km.

From Table 3, it is clear that the maximum payload would be achieved using the highest staging velocity possible. The limitation of the staging velocity was the ability of the vehicle to glide back to the launch site after staging. This maximum velocity from which a return to launch site glide was possible was found to be approximately 1200 m/s, corresponding to a Mach number of 3.9.

When comparing this value to the value used by Powell et al.,[9] it was found to be considerably higher. Powell et al.[9] chose a staging Mach number of three to allow a glide return flight to the launch site. This low staging velocity made an allowance for a safety factor with respect to the glide distance and was also low enough to limit aerodynamic heating. Low aerodynamic heating eliminated the requirement for a thermal protection system (TPS) on the booster stage. The present study allowed for the mass of a TPS on the booster, thereby allowing higher heating loads and possibly accounting for the higher staging Mach number.

Design Point Vehicle

The design point for this concept was a 1200 m/s staging velocity. The flight-path angle at this staging condition was found to be optimal at a value of 27 deg for the powered ascent flight. The vehicle would consist of the same parallel, propellant cross-feed, winged, two-stage configuration used earlier. The booster would employ six AJ26-59 rocket engines and would have a liftoff mass of 769 tons, whereas the orbiter would have five AJ26-60 engines and a liftoff mass of 631 tons.

As Figs. 8 and 9 show, the vehicle would accelerate to a velocity of 1200 m/s and an altitude of approximately 30 km. It would then separate, and the orbiter would continue along its ascent trajectory while the booster began its unpowered return flight to the launch site.

From Fig. 9 it is apparent that the vehicle in the mated configuration would produce only a small portion of the total velocity change

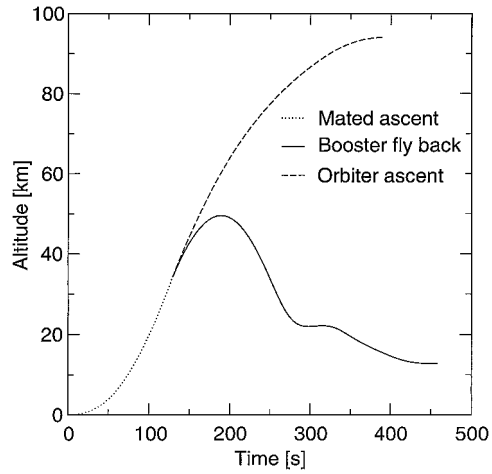

Fig. 8 Gliding booster altitude profile.

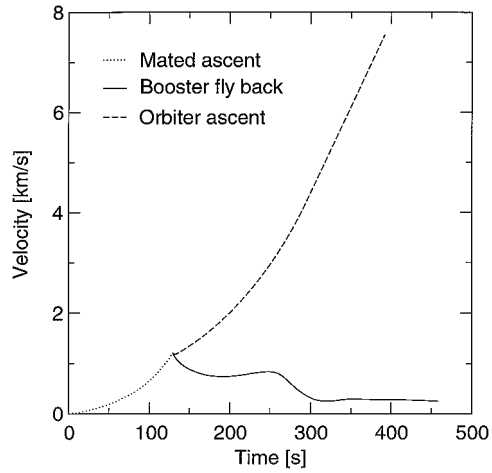

Fig. 9 Gliding booster velocity profile.

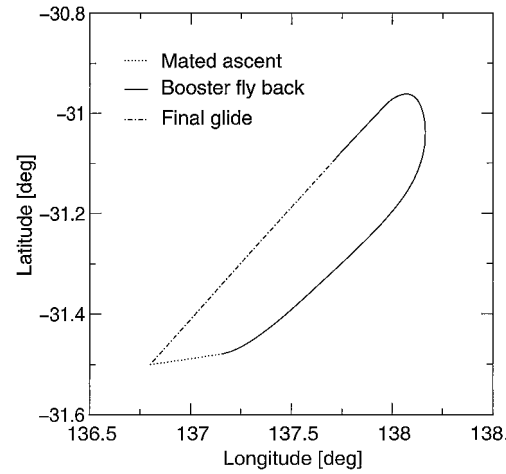

Fig. 10 Gliding booster ground track.

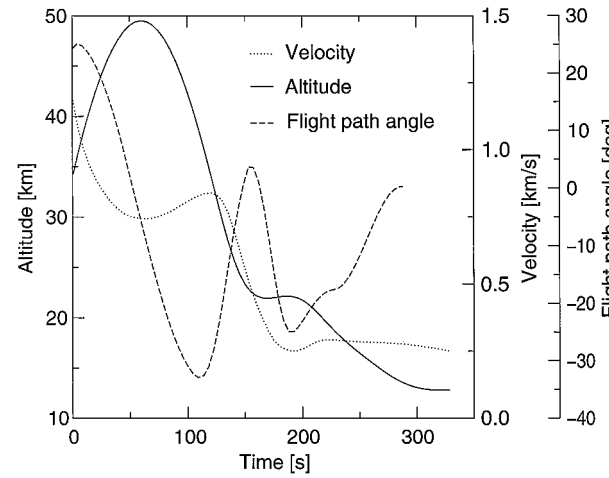

Fig. 11 Gliding booster flyback mission.

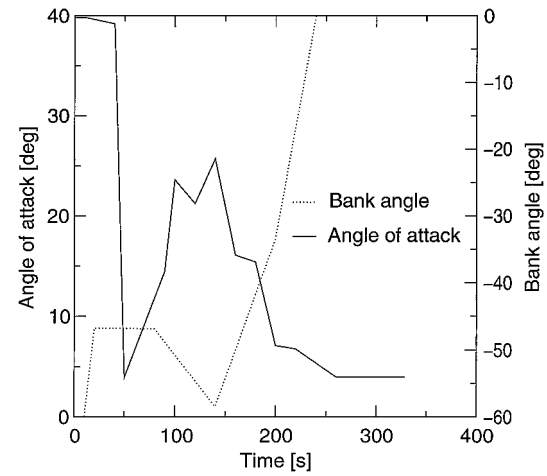

Fig. 12 Gliding booster control parameters.

required for the mission. The remaining velocity change necessary would be performed by the orbiter stage alone, thereby making it significantly larger than that for the vehicle with a 3000-m/s staging velocity. As before, the engines on the orbiter would be throttled for the last 95 s of the ascent flight to limit the acceleration of the vehicle.

From Fig. 10, note that after separation, the booster would complete a turn maneuver to assume a heading toward the launch site. The booster would then glide a further 8 km before the optimization was terminated at a velocity of 270 m/s and flight-path angle of 0 deg. It was assumed that the vehicle glide phase, after termination of the optimization, would be at an angle of attack that would maximize the return flight distance. During the first 30 s after separation, the results of Fig. 10 show that a slight heading change would occur. This heading change would be due to the staging occurring at an altitude with a relatively dense atmosphere. This would allow a partial turn maneuver to be executed before the vehicle coasted into the lower atmospheric density region. In this low-density region, a straight flight is observed, as would be the case for the powered booster flight.

Unlike the velocity profile for the powered booster flyback mission, Fig. 11 shows that the booster would begin decelerating immediately after separation. This deceleration would be due to the atmospheric density being relatively high in this region, thereby producing high aerodynamic drag on the vehicle. The aerodynamic drag at the time of staging would be approximately 164 MN. Figure 11 also shows a sharp peak in the flight-path angle between 130 and 220 s flight time. This skip behavior would be caused by the rate of density increase being faster than the deceleration rate, causing increased lift and the leveling out of the altitude profile. Imposing an upper limit on the flight-path angle during the descent stage could minimize the skip. Again, trajectory optimization was terminated when the velocity and flight-path angle constraints were met close to the desired altitude.

As with the control model for the powered return flight design, an arbitrary initial bank angle of −60 deg was used before the activation of the optimization (Fig. 12). In the region of 145 s, there is a peak in the angle-of-attack parameter before it steadily reduces to a constant value of 4 deg. This increase would be required to account for the loss of lift due to the high bank angle, which would be at a value of −58 deg in this flight region.

Comparison

After the two vehicle concepts had been optimized, they were compared on a performance and operational basis to determine which vehicle would best suit commercial requirements. It was decided not to refine the optimum trajectories any further because the changes made were found to have little effect on the payload placed into orbit.

Powered Return Concept

As was seen earlier, a higher staging velocity resulted in a higher payload to orbit. Because of this, the powered return flight concept vehicle was found to be capable of delivering 50% more payload to orbit than the unpowered return concept vehicle.

A powered vehicle would also have significantly more operational flexibility and would be able to land at a range of landing sites in the case of an emergency. This would lead to improved safety for the mission as well as reduced risk of losing the vehicle and payload in the event of the launch site not being available for landing. The initial cost of this concept vehicle would be higher than that for the unpowered return concept vehicle due to the added hardware and complexity of airbreathing engines. The operational costs would also be higher due to servicing and maintaining the airbreathers. It is believed, however, that the higher income due to the improved payload capability would outweigh the extra component and operational costs.

Unpowered Return Concept

This concept is likely to have lower vehicle costs as well as lower operational costs due to the absence of airbreathing engines on the booster. There would, however, be considerable logistical limitations. The full glide potential of the vehicle would not be exploitable due to the safety implications. A considerable factor of safety would have to be applied to the flyback distance in case the vehicle encountered unexpected weather conditions or some other external influence reducing its glide capability. The vehicle would also be limited by the number of landing sites it could fly to in the event of the launch site not being available for landing. The most significant disadvantage of this concept is its inability to exploit high staging velocities, which support higher payload capabilities. This is due to the limited flyback capability of the booster.

Design Choice

When considering the two concepts discussed in this paper, it was decided to choose the vehicle employing airbreathing propulsion for the return flight. Although this vehicle would be more complex and have higher operational costs, the payload advantages seem to be significant enough to make it the preferred design concept. For servicing GTO missions, it is recommended that the vehicle use an expendable kick stage. Table 4 shows the mass distribution for the powered return flight concept vehicle.

Table 4 Mass breakdown in metric tons

Description	Booster	Orbiter
Base structure and tanks	22.2	8.3
Aerodynamic surfaces	3.7	6.1
TPS	4.4	6.4
Propulsion	16.2	3.1
Auxiliary systems	14.7	10.3
Uncertainties	4.9	3.3
Dry mass	65.1	37.5
Propellants	1039	209
Payload	277	21.6

Conclusions

It can be concluded that the optimal staging conditions for a two-stage reusable vehicle is at approximately 3000 m/s for a powered return flight and approximately 1200 m/s for an unpowered return flight. Furthermore the staging velocity for an unpowered flyback concept should be as high as possible, while still being low enough to allow a safe return glide flight to the launch site.

The investigation also indicated that for a staging velocity of 3000 m/s, it would not be advantageous to employ stronger and heavier wings to allow for a high load turn during flyback. The added wing weight would outweigh the payload gains obtained by a high load turn. It would, therefore, be beneficial to design the wings for loads encountered during landing and then limit the loading during the flyback maneuver.

It is the view of the authors that the optimal design for a reusable launch vehicle would be to employ a powered flyback booster. There would be additional costs and complexity with the powered vehicle due to the inclusion of airbreathing engines; however, it is believed that these would be compensated for by the significantly improved payload capability. A further suggestion is the use of an expendable kick stage to achieve GTO. This would limit the mass that would need to be accelerated to orbit, thereby increasing the GTO payload capability.

Acknowledgments

We would like to thank the Sir Ross and Sir Keith Smith Fund for providing funding for the research. We would also like to thank the Space Systems Institute, University of Stuttgart, for the use of their software and computing services.

References

[1] Isakowitz, S. J., *International Reference Guide to Space Launch Systems*, 2nd ed., AIAA, Washington, DC, 1995.

[2] Middleton, B. S., "The Global Space Launch Market in the Next Decade," International Aerospace Congress, Paper IAC-99-NS 4.7, Sept. 1999.

[3] "FESTIP System Concepts Description," TR, Daimler–Benz Aerospace, Ottsbrunn/Munich, Germany, Aug. 1998.

[4] Freeman, D. C., Tally, T. A., Stanley, D. O., Lepsch, R. A., and Wilhite, A. W., "Design Options for Advanced Manned Launch Systems," *Journal of Spacecraft and Rockets*, Vol. 32, No. 2, 1995, pp. 241–249.

[5] Kamody, J. F., Damiani, A., and Stadelman, R. J., "Use of FRP with Alcohol-Containing Fuels," *Journal of Reinforced Plastics and Composites*, Vol. 13, No. 3, 1994, pp. 213–236.

[6] Rahn, M., Schöttle, U. M., and Messerschmid, E., "Impact of Mission Requirements and Constraints on Conceptual Launch Vehicle Design," *Aerospace Science and Technology*, Vol. 3, No. 6, 1999, pp. 391–401.

[7] Chakroborty, S. P., Limerick, C., and Stark, R., "A Systematic Approach for the Development of the Propulsion System for the K-1 Reusable Launch Vehicle," 49th International Astronautical Federation, Paper IAF-98-s.1.08, 1998.

[8] Schöttle, U. M., "Mission Dependend [sic] Selection of Propulsion Systems for Reusable Launch Vehicles," European Aerospace Conf., Paper EAC 89-33, May 1989.

[9] Powell, R. W., Naftel, J. C., and Cruz, C. L., "Ascent Performance Issues of a Vertical Takeoff Rocket Launch Vehicle," *Journal of Spacecraft and Rockets*, Vol. 28, No. 2, 1991, pp. 179–183.

J. A. Martin
Associate Editor